Anal. Chem. **2004,** *76,* 3018−3022

Recirculation of Nanoliter Volumes within Microfluidic Channels

Rob G. H. Lammertink, Stefan Schlautmann, Geert A. J. Besselink, and Richard B. M. Schasfoort*

Biochip Group, MESA+ Research Institute, University of Twente, P.O. Box 217, 7500 AE Enschede, The Netherlands

A microfluidic device is described, capable of recirculating nanoliter volumes in restricted microchannel segments. The device consists of a PDMS microfluidic structure, reversibly sealed to a glass substrate with integrated platinum electrodes. The integrated electrodes generate electroosmotic flow locally, which results in a cycling flow in the channel segment between the two electrodes in case one channel exit is closed (dead-end channel). This cycling flow is a consequence of the counterbalancing hydrodynamic pressure against the electroosmotically generated flow. Acid−base indicators were employed to study the formation of H^+ and OH^- at both the in-channel electrodes. The formation of acid can locally change the zeta-potential of the channel wall, which will affect the flow profile. Using this method, small analyte volumes can be mixed for prolonged times within well-defined channel segments and/or exposed to in-channel sensor surfaces.

Research on microfluidic structures is strongly rising within areas such as analytical (bio)chemistry. So-called, microscale total analysis systems (μTAS) incorporate a number of different preparative and analytical functions within small, often disposable, units.[1] Because of the small dimensions, low Reynolds-numbers exist and turbulence is absent. Within these systems, laminar flow dominates and mixing of materials between streams is purely diffusive and typically requires long channel distances ($\gg$1 cm). Different strategies to increase the mixing efficiency in microchannels have been proposed. Passive mixers typically employ channel geometry to increase the interfacial area between liquids to be mixed. Stroock et al.[2,3] used ridged walls in microchannels in order to generate transverse flows. Another approach involves the use of three-dimensional serpentine microchannels to enhance fluid mixing.[4]

Droplet based microfluidics is a different approach to solve the mixing problem.[5] Using immiscible fluids in microchannels, droplets (plugs) are formed. The droplets consist of aqueous solutions that can contain multiple reagents. Such a droplet develops a recirculating flow within itself when displaced in a microchannel.[6] This recirculating flow enhances mixing by reducing the striation length.[7,8] However, it can only be sustained by continuous drop movement, which either requires long channels or alternating flow directions.

Here, we report on the design and operation of a microfluidic device, capable of establishing a recirculating flow inside an immobile volume. The recirculation is electroosmotically driven by an electrical field obtained from integrated electrodes. An advantage of efficient recirculating flow inside microfluidics is that short channel structures can be used, and consequential, small sample and reagent amounts are needed before homogeneity is attained. For instance, when following binding kinetics between dissolved antibodies and immobilized antigens or when immobilizing biomolecules,[9] it may require 10 min of reaction time or even more. When such reactions are done in a microfluidic format, a circulating flow within a small volume is more desirable than a continuous flow. Besides that, the described microfluidic device may be desirable when only very small sample volumes (nanoliters) are available. One could think of an isolated component (peak) from a microfluidic or capillary separation. These components can elute within typical volumes of about 10 nL and can be further processed by the described microfluidic unit (binding, (de)staining, reaction, etc.).

EXPERIMENTAL SECTION

Electrodes were fabricated on glass via a deposition and lift-off process. First, a photoresist is spin-coated onto the glass substrate, exposed, and developed. Then a 10 nm layer of chromium is deposited on the glass/photoresist substrate, followed by a 100 nm platinum layer. Lift-off of the photoresist by ultrasonic cleaning in acetone leaves the electrode structure behind on the glass substrate.

Microfluidic structures were fabricated by a replication method. First, a master was fabricated using SU-8 photoresist on a silicon wafer. Poly(dimethylsiloxane) (PDMS, Sylgard 184, Dow Corning) (10 parts base to 1 part curing agent) was poured onto the wafer and cured for 3 h at 70 °C. After curing, the PDMS slab was peeled off and individual devices were cut out. The channels were 50 μm wide and approximately 100 μm high. As can be seen from

* Corresponding author. Phone: 31-53-4895621. Fax: 31-53-4891105. E-mail: r.b.m.schasfoort@utwente.nl.

(1) Van den Berg, A.; Bergveld, P. *Micro Total Analysis Systems*; Kluwer Academic Publishers: London, 1995.
(2) Stroock, A. D.; Dertinger, S. K. W.; Ajdari, A.; Mezić, I.; Stone, H. A.; Whitesides, G. M. *Science* **2002**, *295*, 647−651.
(3) Stroock, A. D.; Dertinger, S. K.; Whitesides, G. M.; Ajdari, A. *Anal. Chem.* **2002**, *74*, 5306−5312.
(4) Liu, R. H.; Stremler, M. A.; Sharp, K. V.; Olsen, M. G.; Santiago, J. G.; Adrian, R. J.; Aref, H.; Beebe, D. J. *J. Microelectromech. Syst.* **2000**, *9*, 190−196.
(5) Tice, J. D.; Song, H.; Lyon, A. D.; Ismagilov, R. F. *Langmuir* **2003**, *19*, 9127−9133.
(6) Duda, J L.; Vrentas, J. S. *J. Fluid Mech.* **1971**, *45*, 247−260.
(7) Handique, K.; Burns, M. A. *J. Micromech. Microeng.* **2001**, *11*, 548−554.
(8) Hosokawa, K.; Fuji, T.; Endo, I. *Anal. Chem.* **1999**, *71*, 4781−4785.
(9) Delamarche, E.; Bernard, A.; Schmid, H.; Michel, B.; Biebuyck, H. *Science* **1997**, *276*, 779−781.

10.1021/ac0353942 CCC: $27.50
Published on Web 05/04/2004

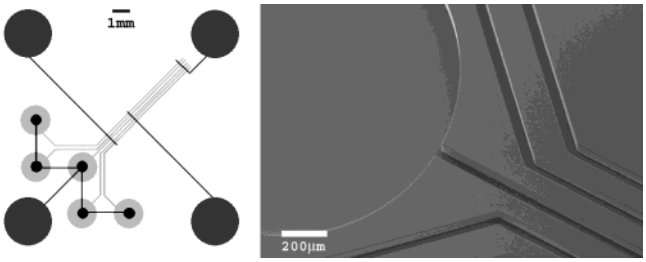

Figure 1. Schematic illustration and scanning electron micrograph of a microfluidic and electrode layout. In the left image, the dark gray features correspond to the platinum electrodes with large round wire contact areas in each corner. The light gray features correspond to the microfluidic structures, comprising five inlet reservoirs and dead-end channels. The right image displays a part of the channels and one inlet reservoir.

the SEM image in Figure 1 the channels have straight sidewalls. Holes for fluid reservoir and electrode access were punched through the PDMS using a blunt needle. The PDMS and glass slides were rinsed with ethanol and brought into contact prior to drying. Using an inverted microscope or a stereomicroscope, the microfluidics could be aligned by hand with respect to the platinum electrodes. After assembly the chips were dried at room temperature. This method did not involve any oxidative treatment of the PDMS and therefore results in a reversible seal between the PDMS and glass substrate.

Dead-end channels can be filled with aqueous solutions by immersing the complete chip and placing it under reduced pressure for some minutes.[10] A 10 mM $NaHCO_3$ buffer (pH 9.0) was used in all experiments, unless indicated otherwise. The chips were placed in a holder that incorporates the electrical contacts. The voltages were supplied by an EOF control unit (IBIS CU 411, IBIS Technologies Hengelo, The Netherlands).

Bovine serum albumin (BSA) and fluorescein isothiocyanate (FITC) were obtained from Sigma (St. Louis, MO). "Uniform Dyed Microspheres" (type PS yellow fluorescent, diameter 2.60 μm, 10% w/v) were obtained from Bangs Laboratories, (Fishers, IN). All the other chemicals were purchased from VWR International GmbH (Darmstadt, Germany) and were of analytical grade. BSA was fluorescently labeled by treatment for 30 min at room temperature with (a 60-fold molar excess of) FITC in 0.5 M sodium borate, pH 9.0, followed by gel filtration over a PD-10 column. An inverted microscope (Olympus IX51), equipped with fluorescence unit and an F-View II 12 bit CCD camera, was used to view device operation.

Simulations were carried out using CFD-ACE+ software (CFD Research Corp.). Three-dimensional channels with walls having different zeta-potential, to simulate the PDMS-glass hybrid chips, and integrated electrodes were employed using the finite volume method. The electroosmotic mobilities used for glass and PDMS were 7.0×10^{-4} and 3.5×10^{-4} $cm^2/(V \cdot s)$, respectively (rounded numbers based on EOF measurements in glass and PDMS devices).

RESULTS AND DISCUSSION

For our experiments we assembled microfluidic chips, consisting of a glass wafer substrate with platinum electrodes onto which a PDMS microfluidic layout was placed (see Figure 1). As a result, the corresponding microchannels consisted of one glass wall and three PDMS walls. Recently, PDMS has received considerable attention and shows particular promise for the design and fabrication of microfluidic devices.[11,12] The PDMS formulation used throughout this research supports electroosmotic flow in its native form. This, and the pH dependence of EOF found in these devices, can be explained by the silica filler particles used in this formulation.[13] Although it is possible to modify the PDMS surface to control surface charge[13,14] we employ PDMS in its native form.

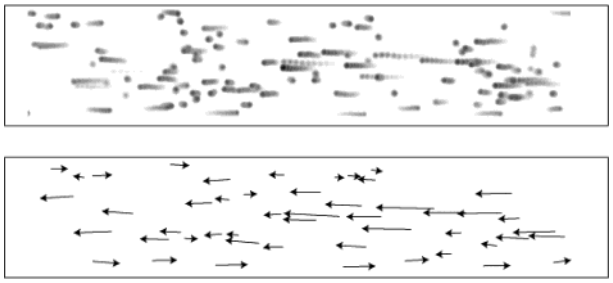

Figure 2. Visualization of flow in a segment of the dead-end channel, using fluorescent PS beads. A positive potential was applied at the left side of the imaged microchannel area. Along the wall, the beads move in the direction of the EOF.

By applying a potential across a section of a microchannel, electroosmotic flow is generated between the active electrodes. In a channel of which one end is closed (dead-end channel), the generated electroosmotic flux is counterbalanced by a hydrodynamic flux. Therefore, the velocity profile becomes a superposition of a plug flow and a Poiseuille flow in opposite directions. This means that fluid flows along the wall in the direction of the EOF and reverses through the middle of the microchannel. Figure 2 displays a schematic representation of observations on beads flowing inside a dead-end channel segment, by the application of a local electric field. The focus of the microscopic image corresponds to the center of the channel and therefore corresponds to a longitudal cross section of the microfluidic channel. Beads flowing near the upper and lower channel wall are therefore out of focus and are not observed in the image. It is clear that near the side walls the fluid moves in an opposite direction compared to the fluid in the center of the channel.

To get a good impression about the flow profile inside the microchannel, simulations were carried out. From the results of the simulations (Figure 3) it can be seen that the fluid moves in the EOF direction near the channel wall and back through the middle of the channel. The maximum flow velocities near the channel walls correspond to the electroosmotic mobilities of glass and PDMS in open channel structures. The values for the electroosmotic mobilities used for the simulations only affect the magnitude of the flow velocity near the channel wall. This is a consequence of the superposition of the flow profiles, where the opposite Poiseuille flow is zero at the channel wall. One advantage

(10) Monahan, J.; Gewirth, A. A.; Nuzzo, R. G. *Anal. Chem.* **2001**, *73*, 3193−3197.
(11) Duffy, D. C.; McDonald, J. C.; Schueller, O. J. A.; Whitesides, G. M. *Anal. Chem.* **1998**, *70*, 4974−4984.
(12) McDonald, J. C.; Duffy, D. C.; Anderson, J. R.; Chiu, D. T.; Wu, H.; Schueller, O. J. A.; Whitesides, G. M. *Electrophoresis* **2000**, *21*, 27−40.
(13) Ocvrik, G.; Munroe, M.; Tang, T.; Oleschuk, R.; Westra, K.; Harrison, D. J. *Electrophoresis* **2000**, *21*, 107−115.
(14) Liu, Y.; Fanguy, J. C.; Bledsoe, J. M.; Henry, C. S. *Anal. Chem.* **2000**, *72*, 5939−5944.

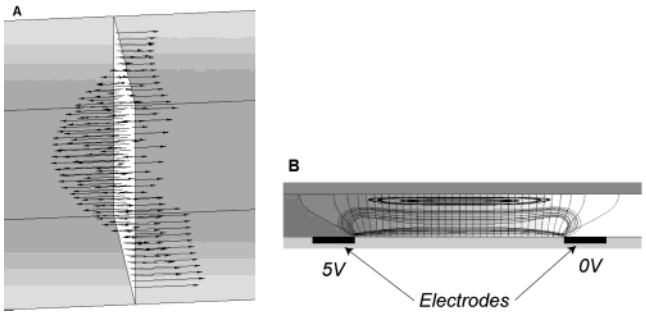

Figure 3. CFD simulation results of electroosmotically driven flow in a closed channel. The bottom channel wall consists of glass, where the other three channel walls are composed of PDMS. A. The flow velocity profile is depicted. B. Flow traces and isopotential lines illustrate the confined circulating volume and localized electrical field.

of the different flow velocities at the individual channel walls (glass versus PDMS) is that the dispersion rate within this restricted volume will be increased which is beneficial for efficient mixing. Since EOF is only present between the active electrodes used to apply the potential, the flow is localized within that segment of the microchannel. Outside of the electrode-bound volume, almost no electrical field is present as can be seen from the isopotential lines in Figure 3.

The situation described above is therefore quite similar to recirculating streamlines in a moving discrete drop. In our case, however, the recirculation is driven by the electroosmotic flow generated between the integrated electrodes and the plug is not moving. The modeling of the mixing within the plug, on the other hand, is analogous to the moving drop situation.[7] In our case the convective transport time scale, t_{conv}, is given by

$$t_{conv} \sim \frac{L}{v} = \frac{L}{\mu_{EO}\vec{E}} = \frac{L^2}{\mu_{EO}V} \qquad (1)$$

where L is the distance between the integrated electrodes, v is the fluid velocity at the channel wall, μ_{EO} is the electroosmotic mobility, the electrical field $\vec{E}$, and V is the applied voltage. On the other hand, the diffusion time scale, t_{diff}, can be estimated by

$$t_{diff} \sim \frac{d^2}{4D} \qquad (2)$$

where d is the channel diameter, and D is the diffusion coefficient. For convection controlled mixing, t_{conv} should be less than t_{diff}. This results in a simple relation for the required applied voltage where convective mixing dominates:

$$V_{min} > \frac{4L^2D}{d^2\mu_{EO}} \qquad (3)$$

As an example, an interelectrode distance of 1 mm, a channel diameter of 50 μm, a diffusion coefficient of 1×10^{-10} m^2/s, and an electroosmotic mobility of 5.0×10^{-4} cm^2/(V·s) (averaging the respective values for glass and PDMS) result in a V_{min} of 3.2 V. Note that the aspect ratio of the recirculating volume (L/d) quadratically affects the minimum voltage required for convective mixing. Therefore, V_{min} can be easily further reduced by decreasing the distance between the electrodes or increasing the microchannel diameter.

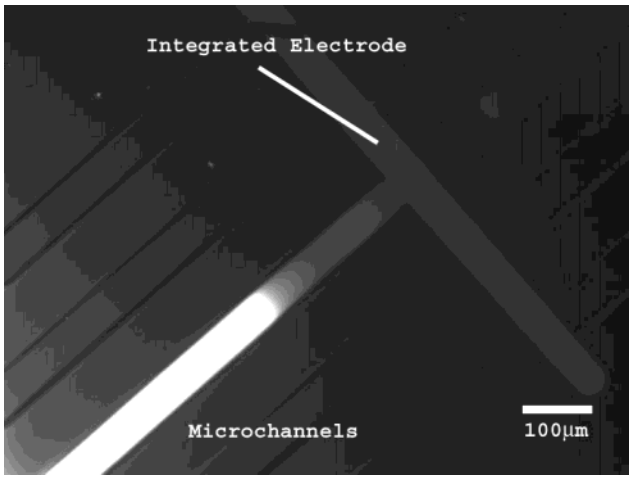

Figure 4. Fluorescent micrograph of the device during operation with fluorescently labeled BSA as a marker. A 3 V potential was applied to the integrated Pt electrode, 1.3 mm separated from the grounded electrode (23 V/cm) which is located toward the lower left side, out of the field of view.

Subsequently, fluorescently labeled BSA (bovine serum albumin) was used as a marker inside the microchannel. From Figure 4 it can be seen that the front of the BSA solution displays a rather sharp boundary near the electrode position. The integrated electrode in this image was held at 3 V, while it was separated 1.3 mm from the grounded electrode (not shown, but at the lower left corner outside the field of view). Besides that, this front slowly moves away from the electrode during device operation. Even when the channel is first filled completely with the fluorescently labeled BSA, a depletion volume develops near the integrated electrode. In the following section we will provide a possible explanation for this phenomenon.

Due to the electrolysis of water, local formation of H^+ at the anode and OH^- at the cathode occurs. Besides that, the oxidation of water results in O_2 gas formation at the anode and H_2 gas formation at the cathode:

anode $\quad 2H_2O \leftrightarrow 4H^+ + O_2 + 4e\text{-}$

cathode $\quad 4H_2O + 4e^- \leftrightarrow 4OH^- + 2H_2$

Basically, this means that for every electron one H^+ and OH^- are formed at the corresponding electrodes. The conductivity of a 10 mM $NaHCO_3$ buffer is approximately 1.0 mS/cm, which results in 1 μA current when 2 V is applied across an electrode distance of 1 mm. For 1 μA of current, this implies that about 10^{-11} mol of H^+ and OH^- are formed every second. In a 10 nL volume this is about 10^{-3} M/s. These are substantial acid and base productions that will affect the local pH. To study the acidification within the microchannel, acid−base indicators were used. Due to the short interelectrode distance, relatively low voltages can be applied in order to generate significant electrical fields and hence velocities.

Figure 5 illustrates the acid formation at the positive electrode during the device operation, using 10 mM $NaHCO_3$ (pH 9.0) as a

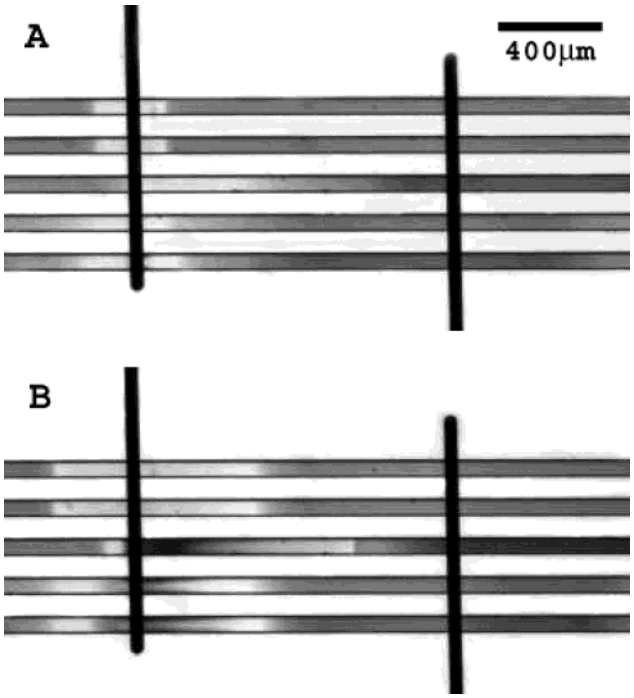

Figure 5. Micrographs of a 5-channel device with two integrated electrodes, filled with different acid−base indicators. After applying 3 V (A) or 4 V (B) to the integrated left electrode for 30 s, acid is formed at this electrode. The integrated right electrode was grounded in all cases. The upper 2 channels contain phenol red, and the bottom 3 channels (3−5) contain thymol blue. The middle channel is the only open channel; all others are dead-end channels.

buffer. The top two channels are filled with phenol red (indicator colors: light yellow at pH<6.4, dark red at pH>8.0), and the bottom three channels with thymol blue (indicator colors: dark red at pH <1.2, light yellow between pH 2.8 and pH 7.8, dark blue at pH>9.5). When a voltage of 3 V is applied to the left electrode and 0 V to the right electrode (resulting in a local 25 V/cm field), color changes are rapidly and clearly apparent (see Figure 5A). The phenol red displays a rather sharp boundary, indicating a local pH of 6.4−8.0, close to the electrode. The thymol blue transition between yellow and blue, indicating a local pH of 7.8−9.5, is somewhat further separated from the electrode and less sharp. When applying higher voltage (4 V, Figure 5B) acid is formed faster. Near the electrode, even the transition between dark red and yellow appears for thymol blue, indicating a pH < 1.2 locally. The middle channel in both images (Figure 5A,B) is the only channel of which both ends are open. This results in an electroosmotic flow that transports the acid formed at the electrode along through the microchannel. The continuous acid production at the left electrode will result in acidification of the complete microchannel segment that is bordered by the electrodes, as is evident from Figure 5. Contrastingly, this indicates that the fluid circulation within a dead-end microchannel segment results in some neutralization of the acid and base production.

As mentioned before, the pH may locally drop to values below 1.2, as a result of in-channel acid production. Already at pH values below 3.0 the EOF in PDMS will diminish.[13] In the vicinity of the electrode, there exists a region where fluid circulation becomes limited (see Figure 6). The fluid only circulates within the part of the channel where surface charges, and therefore EOF, are

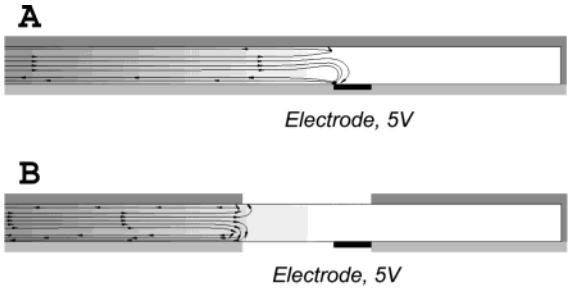

Figure 6. CFD simulation results. A. The starting situation, where the complete channel is charged and supports EOF. B. The situation where a part of the channel does not support EOF (indicated as white), and hence the circulating flow is expelled from this area. A clear transition between circulating and noncirculating volumes exists.

present. This phenomenon becomes more apparent when voltages are applied for longer times. Reduced fluid circulation in the acidifying regions results in more acid accumulation and hence a more dramatic pH drop. On the other hand, when using 100 mM $NaHCO_3$ as a buffer, there is very little change in the pH locally when applying similar voltages to the ones displayed in Figure 5. The generation of gas is then greater, due to the increased current, and this will lead to bubble formation sooner (already at about 5 V).

Local protonation of the channel walls at low pH values results in low localized zeta-potentials. Spatial- and time-controlled modification of the zeta-potential is therefore possible, similarly to the field-effect flow control.[15] Within the volume near the positive integrated electrode, there is very limited fluid flow, and hence the pH drop becomes quite significant in time due to ongoing acid production. The effect as displayed in Figure 4 can therefore be explained by the reduced quantum yield of fluorescein under acidic conditions.[16]

Although the demonstration of the device operation was performed in a dead-end channel, from a practical point of view, open channels are more desirable. Using the same principle, it is very straightforward to design open channel structures that will generate recirculating flow within immobilized volumes. One approach is the use of an even number of volume segments in series, where each volume segment has an opposite circulating direction compared to the neighboring one. In other words, the EOF generated by each volume is counterbalanced by the EOF generated by the neighboring volume. This can be established by employing an uneven number of electrodes, with a certain potential applied to all even ones while keeping all odd ones grounded. The principle is demonstrated in Figure 7.

The application of high voltages to the in-channel electrodes, or the use of more conducting buffer solutions, will result in excessive gas formation at both electrodes and thereby in failure of the experiment. We need to stress, however, that PDMS fabricated devices tolerate little gas formation since the gas can diffuse out of the microchannel through the PDMS matrix material.[17] However, as already indicated by Ramsey et al.[17] the

(15) Schasfoort, R. B. M.; Schlautmann, S.; Hendrikse, J.; van den Berg, A. *Science* **1999**, *286*, 942−945.

(16) In additional experiments we measured the fluorescence intensities of fluorescein labeled BSA at different pH values. The observed reduction in fluorescence was found to be adequate in explaining the formation of a (fluorescence) depletion volume.

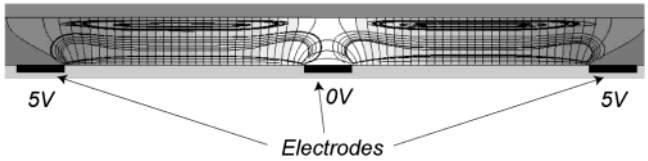

Figure 7. CFD simulation results of two volume segments in an open channel, having opposite circulation directions. There is no net fluid flow through the open channel.

gas permeability for PDMS is too low to account for the expected gas generation by electrolysis. They stated that the fluid flow may sweep away electrolysis products from the electrode region down the channel, thereby increasing the effective permeable surface. Furthermore, they proposed the use of other (then gold) electrode materials to reduce the gaseous electrolysis production. For the devices described in this paper, platinum was used as electrode material. Initial experiments were carried out with gold electrodes, but this was found to result in device failure by gas bubble formation much sooner. In our experiments, voltages up to 5 V could be applied when using 100 mM $NaHCO_3$ buffer solution, resulting in a stable device operation without observable gas formation. For lower buffer concentrations, even higher potentials are tolerable.

(17) McKnight, T. E.; Culbertson, C. T.; Jacobson, S. C.; Ramsey, J. M. *Anal. Chem.* **2001**, *73*, 4045−4049.

CONCLUSIONS

We have demonstrated the operation of a microfluidic device, capable of circulating nanoliter volumes in restricted channel segments. Due to the use of in-channel electrodes, the application of somewhat permeable materials, such as PDMS, is desired for fabrication. Operation of the device results in acid and base formation at the corresponding electrodes. This may result in local protonation of the channel wall, locally reduced EOF, and therefore altered flow inside the microchannel. When using relatively low electrical potentials, good long-term operation can still be obtained without a dramatic pH change at the electrodes. Higher buffer concentration also results in less dramatic pH changes but leads to detrimental gas formation sooner. The described device operation is also applicable in open channel structures. In that case, counter rotating volume segments are placed in series. This makes the described system very suitable to study a large number of batch processes simultaneously.

Received for review November 25, 2003. Accepted February 26, 2004.

AC0353942